A numerical study on prediction of ship maneuvering in waves

ZHANG Wei[1], ZOU Zaojian[1,2]

1. School of Naval Architecture, Ocean and Civil Engineering; 2. State Key Laboratory of Ocean Engineering,

Shanghai JiaoTong University, Shanghai 200240, China

(drwood@sjtu.edu.cn zjzou@sjtu.edu.cn)

Highlights:

- A numerical method is developed for predicting ship maneuvering in waves, based on the two-time scale model.
- The linear hydrodynamic forces on the maneuvering hull are evaluated based on the double body model with a trailing vortex sheet, and the effects of the trailing vortices on the wave forces are considered indirectly.
- The present method is validated by comparing the numerical results with the free running model test data.

1 Introduction

Prediction of ship maneuverability is typically carried out in clam water conditions. This gives valuable information at the ship design stage. However, an actual seagoing ship usually maneuvers in the presence of waves. From the viewpoint of ship safety, it is meaningful to understand the maneuvering behavior of a ship in waves.

To study the maneuverability of a ship in waves, combining the theories of maneuvering and seakeeping is needed. A practical combining approach is to use the two-time scale model, which separates the basic motion equations into two groups: the one for high frequency wave-induced motion and the other for the low frequency maneuvering motion. Typical works in this area have been reported by Skejic and Faltinsen [1], Yasukawa and Nakayama [2] and Seo and Kim [3].

In the present study, numerical simulations of the ship maneuvering in waves are carried out. The maneuvering motion is calculated using 4-DOF MMG model, whereas the wave-induced motions are determined by solving a linearized boundary value problem (BVP) in time domain. The maneuvering and seakeeping problem is integrated by a two-time scale model, following the approach of Seo and Kim [3]. Numerical results for the S-175 container ship turning in waves are presented and compared with experimental data to validate the numerical method.

2 Mathematical formulations

2.1 *Coordinate systems*

Two coordinate systems are adopted, as shown in Fig. 1. The first one $\bar{x} = (x, y, z)$ is body-fixed, with the positive x towards the bow and the positive z pointing upward. The xy plane is coincident with the calm water level and the origin of the frame is at the midship; the second one $\bar{X} = (X, Y, Z)$ is fixed in space.

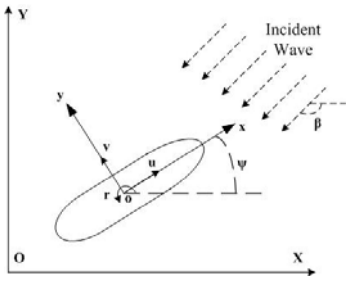

Fig. 1 Coordinate systems

2.2 *Basic motion equations*

The ship is assumed rigid and undergoing six degrees of freedom oscillations while translating with forward speed u, transverse speed v and rotating with yaw rate r in regular waves. Based on the two-time scale model, ship motion is assumed to be the sum of the high frequency wave-induced motion and the low frequency maneuvering motion.

The 6-DOF motion equations for high frequency problem are expressed as:

$$[M_{ij}]\{\ddot{\xi}_j(t)\} + [C_{ij}]\{\xi_j(t)\} = \{F_i\} \quad (i, j = 1,2\ldots6) \qquad (1)$$

where $\vec{\xi}_T = (\xi_1, \xi_2, \xi_3)$ and $\vec{\xi}_R = (\xi_4, \xi_5, \xi_6)$ represent the ship's translational and rotational displacements, respectively; $[M_{ij}]$ is the inertial matrix for the hull, $[C_{ij}]$ is the matrix of hydrostatic restoring coefficients and $\{F_i\} = (F_x, F_y, F_z, M_x, M_y, M_z)$ denotes the hydrodynamic force and moment for high frequency component. The ship displacement about the body-fixed frame is written as:

$$\vec{\xi} = (\xi_x, \xi_y, \xi_z) = \vec{\xi}_T + \vec{\xi}_R \times \bar{x} \qquad (2)$$

The equations of low frequency ship maneuvering motion

are expressed as:

$$\left.\begin{aligned} &m(\dot{u}-vr-x_G r^2+\dot{\phi}rz_G)=X_H+X_P+X_R+X_W\\ &m(\dot{v}+ur+x_G\dot{r}+\ddot{\phi}z_G)=Y_H+Y_R+Y_W\\ &I_{xx}\dot{p}-mz_G(\dot{v}+ur)=K_H+K_R+K_W\\ &I_{zz}\dot{r}+mx_G(\dot{v}+ur)=N_H+N_R+N_W \end{aligned}\right\} \quad (3)$$

where m is ship's mass, I_{xx} and I_{zz} are moments of inertia. x_G and z_G represent the coordinates of the center of gravity, the subscripts H, P, and R denote the hydrodynamic forces of low frequency motion on the hull, propeller and rudder, respectively; the subscript W denotes the wave drift forces. The hull force $\vec{F}_H=(X_H,Y_H,K_H,N_H)$ can be decomposed as

$$\begin{aligned} X_H&=-m_x\dot{u}+m_y v\dot{\psi}+X_{nonlinear}-R(u)\\ Y_H&=-m_y\dot{v}-m_x u\dot{\psi}+Y_v v+Y_r r+Y_{nonlinear}\\ K_H&=-mg\overline{GM}\sin\phi-K(\dot{\phi})-z_H Y_H\\ N_H&=-J_{zz}\dot{r}+N_v v+N_r r+N_{nonlinear} \end{aligned} \quad (4)$$

where m_x and m_y are the added masses, and J_{zz} and J_{xx} are the added moments of inertia in zero frequency.

In the present study, the linear force ($Y_v v, Y_r r, N_v v, N_r r$), the high frequency force $\{F_i\}$, and the wave drift forces are calculated by solving the BVPs. The rudder, propeller and nonlinear hull force components are obtained from the model test [4].

2.3 *Modeling of hydrodynamic forces*

In order to calculate the hydrodynamic forces in time domain, temporal discretizations must be introduced. Since the frequencies of maneuvering motion and wave-induced motion are very different, two different time scales, denoted by τ_L and τ_H, are used in the low frequency problem and the high frequency problem, respectively. The ratio between τ_L and τ_H is donated by N, which is generally much larger than 1.

During the interval of each maneuvering time step τ_L, the ship speed is assumed to be constant, and is defined as

$$\vec{W}=(u-ry)\vec{i}+(v+rx)\vec{j}+0\vec{k} \quad (5)$$

where $(\vec{i},\vec{j},\vec{k})$ are the unit vectors associated with the ship-fixed coordinates.

Under the assumption that the fluid is inviscid and incompressible, and the flow is irrotational, the fluid velocity potential can be introduced. The total disturbance potential $\Psi(\vec{x},t)$ satisfies the following BVP:

$$\left.\begin{aligned} &\nabla^2\Psi=0 \quad \text{in fluid domain}\\ &(\frac{\partial}{\partial t}-(\vec{W}-\nabla\Psi)\cdot\nabla)[z-\eta(x,y,t)]=0 \quad \text{on z=}\eta(x,y,t)\\ &\frac{\partial\Psi}{\partial t}-\vec{W}\cdot\nabla\Psi+\frac{1}{2}\nabla\Psi\cdot\nabla\Psi=-g\eta \quad \text{on z=}\eta(x,y,t)\\ &\frac{\partial\Psi(\vec{x},t)}{\partial n}=\vec{W}\cdot\vec{n}+\frac{\partial\vec{\xi}}{\partial t}\cdot\vec{n} \quad \text{on body surface} \end{aligned}\right\} \quad (6)$$

where $\vec{n}$ is the inward unit normal on the hull surface.

In addition, for the ship in oblique or turning motion, which can be regarded as a lifting body, a Kutta condition should be imposed at the trailing edge of the hull.

To linearize the free surface boundary conditions, the total disturbance potential Ψ is decomposed into a basis flow $\Phi(\vec{x})$ and a perturbation flow $\varphi_P(\vec{x},t)$:

$$\Psi(\vec{x},t)=\Phi(\vec{x})+\varphi_P(\vec{x},t) \quad (7)$$

The basis flow is assumed to be the main component with its order of $O(1)$ and is related to the double body flow, which includes the one induced by maneuvering motion. To account for the lifting effect associated with the maneuvering motion, trailing vortex sheets are introduced which are assumed shed from the hull at both the keel line and the trailing edge of the hull, as shown in Fig. 2. By referring the work of Matsui et al. [5], a linear trailing vortex sheet is adopted. In the numerical approach, the length of the vortex sheets are assumed to be six times of the ship length and the angle Θ between the x-axis and the free vortex line is determined by the following formula:

$$\Theta=0.5\arctan(v/u) \quad (8)$$

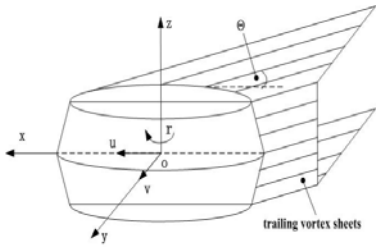

Fig. 2 The vortex model

The perturbation potential $\varphi_P(\vec{x},t)$ and the wave elevation η are assumed to be order of $O(\varepsilon)$. They are decomposed as:

$$\varphi_P(\vec{x},t)=\varphi(\vec{x},t)+\varphi_I(\vec{x},t) \quad (9)$$

$$\eta(x,y,t)=\zeta(x,y,t)+\zeta_I(x,y,t) \quad (10)$$

where $\varphi_I(\vec{x},t)$ represents the incident wave potential, $\zeta_I(x,y,t)$ is the incident wave elevation. $\varphi(\vec{x},t)$ and $\zeta(x,y,t)$ denote the remaining parts of the disturbance potential and wave elevation, respectively.

The linearized BVP for $\varphi(\vec{x},t)$ is written as follows:

$$\left.\begin{aligned} &[\frac{\partial}{\partial t}-(\vec{W}-\nabla\Phi)\cdot\nabla]\zeta=\frac{\partial^2\Phi}{\partial z^2}\eta+\frac{\partial\varphi}{\partial z}-\nabla\Phi\cdot\nabla\zeta_I \quad \text{on z=0}\\ &[\frac{\partial}{\partial t}-(\vec{W}-\nabla\Phi)\cdot\nabla]\varphi=-g\zeta-\nabla\Phi\cdot\nabla\varphi_I \quad \text{on z=0}\\ &\frac{\partial\varphi}{\partial n}=\sum_{j=1}^{6}(\frac{\partial\xi_j}{\partial t}n_j+\xi_j m_j)-\frac{\partial\varphi_I}{\partial n} \quad \text{on } \bar{S}_B \end{aligned}\right\} \quad (11)$$

where $(n_1,n_2,n_3)=\vec{n}$, $(n_4,n_5,n_6)=\vec{x}\times\vec{n}$ and m_j is the so-called m-terms, which are evaluated as

$$\begin{aligned} &(m_1,m_2,m_3)=(\vec{n}\cdot\nabla)(\vec{W}-\nabla\Phi),\\ &(m_4,m_5,m_6)=(\vec{n}\cdot\nabla)(\vec{x}\times(\vec{W}-\nabla\Phi)) \end{aligned} \quad (12)$$

Theoretically, an interaction exists between the trailing

vortices and the disturbance potential $\varphi(\vec{x},t)$. In the present study, however, the influence of the wave potential on the trailing vortices is neglected, because of the difficulty to determine the strength of the vortex in the presence of free surface and incident waves. The error introduced by this treatment is supposed to be small, since $\varphi(\vec{x},t)$ is smaller than $\Phi(\vec{x})$ by an order of magnitude. On the other hand, the effects of the trailing vortices on the wave potential $\varphi(\vec{x},t)$ are considered through the *m*-terms as well as the leading-order terms kept in the free surface boundary conditions.

Using Bernoulli's equation, the hydrodynamic pressure is obtained

$$p^{(0)} = -\rho(\vec{W}\cdot\nabla\Phi + \frac{1}{2}\nabla\Phi\cdot\nabla\Phi) \tag{13}$$

$$p^{(1)} = -\rho(\frac{\partial}{\partial t} - (\vec{U}-\nabla\Phi)\cdot\nabla)\varphi \tag{14}$$

where $p^{(0)}$ and $p^{(1)}$ denote the pressures from the base flow and the perturbation flow, respectively.

The linear forces for low frequency motion satisfy the following equations:

$$Y_v v + Y_r r = \iint_{\bar{S}_B} p^{(0)} n_2 \, ds \tag{15}$$

$$N_v v + N_r r = \iint_{\bar{S}_B} p^{(0)} n_6 \, ds \tag{16}$$

The generalized hydrodynamic force for high frequency motion can be determined by:

$$F_j = \iint_{\bar{S}_B} p^{(1)} n_j \, ds, \quad j = 1,2,\cdots,6 \tag{17}$$

The second-order hydrodynamic force $\vec{F}^{(2)}$ is evaluated by the following equation:

$$\begin{aligned}
\frac{1}{\rho}\vec{F}^{(2)} =& -\iint_{S_{\bar{B}}}[-\vec{W}\cdot\nabla\Phi + \frac{1}{2}\nabla\Phi\cdot\nabla\Phi + gz]\vec{n}_2 ds - \frac{1}{2}\iint_{S_{\bar{B}}}(\nabla\phi\cdot\nabla\phi)\vec{n} ds \\
&-\iint_{S_{\bar{B}}}\left\{\frac{\partial\phi}{\partial t} - (\vec{W}-\nabla\Phi)\cdot\nabla\phi + g\xi_Z + \nabla[-\vec{W}\cdot\nabla\Phi + \frac{1}{2}\nabla\Phi\cdot\nabla\Phi]\cdot\vec{\xi}\right\}\vec{n}_1 ds \\
&-\iint_{S_{\bar{B}}}\left\{\nabla[\frac{\partial\phi}{\partial t} - (\vec{W}-\nabla\Phi)\cdot\nabla\phi]\cdot\vec{\xi}\right\}\vec{n} ds + \frac{1}{2}\int_{WL} g(\eta-\xi_z)^2\vec{n} dl \\
&-\int_{WL}\left\{\nabla[-\vec{W}\cdot\nabla\Phi(0) + \frac{1}{2}\nabla\Phi\cdot\nabla\Phi(0)]\cdot\vec{\xi}\right\}(\eta-\xi_z)\vec{n} dl \\
&-\int_{WL}[-\vec{W}\cdot\nabla\Phi(0) + \frac{1}{2}\nabla\Phi\cdot\nabla\Phi(0)](\eta-\xi_z)\cdot\vec{n}_1 dl
\end{aligned} \tag{18}$$

where $\vec{n}_1$ and $\vec{n}_2$ mean the linear and second-order components of normal vector on the body surface, respectively. Details about Eq. (18) can be found in Joncquez [6]. The mean values of the *x* and *y* component of $\vec{F}^{(2)}$ equal to the wave drift forces X_W and Y_W, respectively. The wave drift moments K_W and N_W are neglected in the present study, because their magnitudes are generally small.

In this study, the linearized BVP (11) is solved by a time domain Rankine panel method, following the approach of Kring [7]; whereas the maneuvering motion equations (3) is solved by a 4th-order Runge-Kutta scheme. Referring to the study by Seo and Kim [3], a parallel time marching scheme is used (See Fig. 3). The linearized BVP (11) is firstly solved for *N* time steps to obtain the wave-induced ship motion as well as the linear forces (Eqs. (15) and (16)) and the wave drift forces. Then the maneuvering motions are simulated for one time step and the resulted ship speed and position are substituted back to update the BVP for the next time step. This cycle is continued until the end of time-marching procedure.

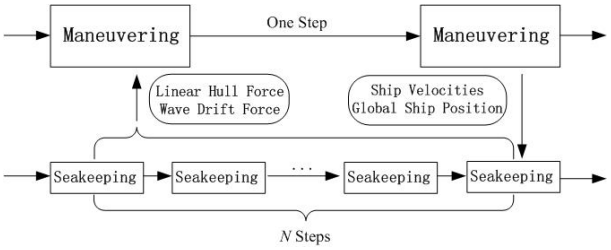

Fig. 3 Time marching scheme

3 Numerical results and discussion

Numerical simulations of the turning tests of the S-175 container ship are carried out, and the numerical results are compared with the data of model tests carried out at the Ocean Engineering Model Basin of Shanghai Jiao Tong University.

Fig. 4 illustrates the comparisons of the turning trajectory in clam water and in waves. It can be seen that the turning trajectories move both along and normal to the wave progress direction. The numerical results can generally give the drift tendency of the turning trajectories, but the predicted turning circles are smaller than those of the experiment. The reason for this difference may be due to the inaccurate evaluation of the mean drift forces.

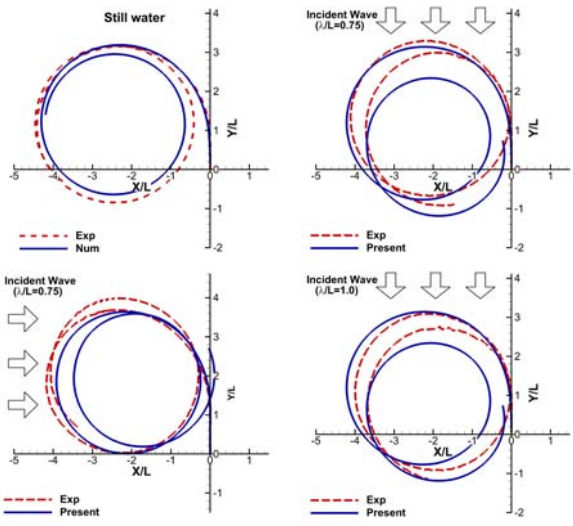

Fig. 4 Comparison of turning trajectories of S-175 model, rudder angle $\delta = 35°$ (port side), wave height $A = 0.01L$.

Fig. 5 illustrates the comparisons of roll and pitch motion when the wave direction $\beta = 180°$. Fig. 6 shows that of $\beta = 90°$. As seen in the figures, the predictions for roll and pitch motion roughly capture the increasing and decreasing of wave-induced motion amplitude associated with turning motion. But a time lag could be found between the predicted motions and the experimental measurements, especially for $t > 60s$. The reasons for this difference may be as follows: The turning period of the S-175 model is about 60*s*. For $t > 60s$, the discrepancies between the numerical prediction of the low frequency motion and the experiment become more remarkable. The poor predictions of the ship turning trajectory result in an error in the encounter frequency of the waves and therefore decrease the prediction accuracy of the wave-induced motions.

4 Concluding remarks

A numerical study on ship maneuvering in waves is carried out, based on the two-time scale model. In order to validate the present numerical method, the turning tests of S-175 model in the presence of waves are simulated. The numerical results are compared with the model test data, which shows that the present method can roughly capture the maneuvering performance of the ship in waves. A further study to improve the present method is still in process.

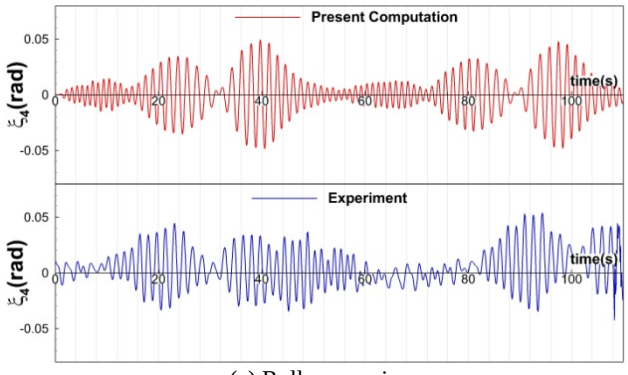

(a) Roll comparison

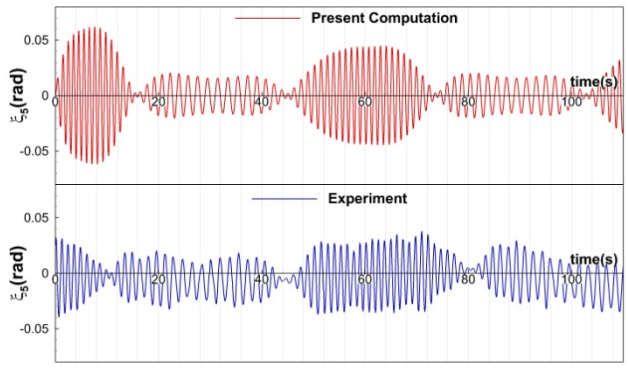

(b) Pitch comparison

Fig. 5 Time histories for S-175 model
($\lambda/L = 1.0,\ A = 0.01L,\ \beta = 180°$)

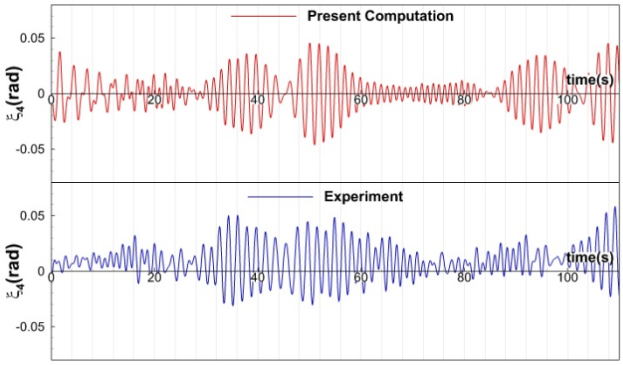

(a) Roll comparison

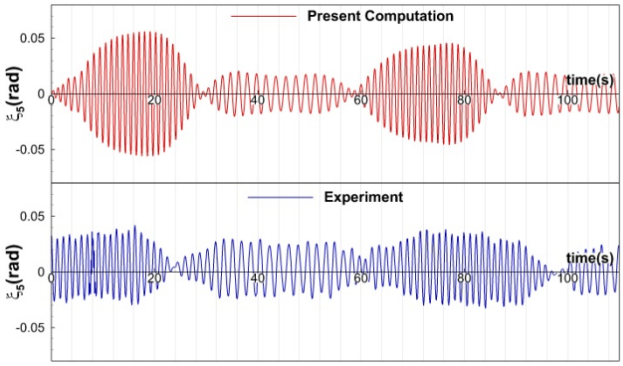

(b) Pitch comparison

Fig. 6 Time histories for S-175 model
($\lambda/L = 1.0,\ A = 0.01L,\ \beta = 90°$)

References

[1] Skejic, R., and Faltinsen, O. M. (2008). A unified seakeeping and maneuvering analysis of ships in regular waves. *J. Mar. Sci. Technol.*, **13**(4), 371-394.

[2] Yasukawa, H., and Nakayama, Y. (2009). 6-DOF motion simulations of a turning ship in regular waves. *Proceedings of MARSIM 2009,* Panama City, Panama.

[3] Seo, M. G., and Kim, Y. (2011). Numerical analysis on ship maneuvering coupled with ship motion in waves. *Ocean Eng*., **38**(17), 1934-1945.

[4] Son, K. H., and Nomoto, K. (1982). On the coupled motion of steering and rolling of a high-speed container ship. *J. Soc. of Naval Arch. and Ocean Eng.*, **20**, 73-83.

[5] Matsui, S., Yang, J., Tamashima, M., and Yoshitake, A. (1994). Calculation of flow around a hull in turning motion and its hydrodynamic forces. *Trans. West-Japan Soc of Naval Arch*, **88**, 13-21.

[6] Joncquez, S. A. G. (2009). Second-order forces and moments acting on ships in waves. Ph.D. Thesis, DTU.

[7] Kring, D. C. (1994). Time domain ship motions by a three-dimensional Rankine panel method. Ph.D. Thesis, MIT.